FLAD-Feature Based Locally Adaptive Diffusion Based Image Denoising

Ajay K. Mandava, Emma E. Regentova, George Bebis*
Department of Electrical and Computer Engineering
University of Nevada, Las Vegas, NV 89154, USA
*Department of Computer Science & Engineering
University of Nevada, Reno, NV 89557, USA
Email: mandavaa@unlv.nevada.edu, emma.regentova@unlv.edu, bebis@cse.unr.edu

Abstract- *A novel patch based adaptive diffusion method is presented for image denoising. This is done with the purpose of locally and feature adaptive diffusion and for attaining patch-wise best peak signal to noise ratio. Our framework uses over-segmentation method to segment the image in to sensible regions and then diffusion of each segment/region to obtain the near-optimal solution and iterates to a lesser-segmented region/patches until a best PSNR value is attained. In performing diffusion the method uses the inverse difference moment (IDM) which is a robust feature in determining the amount of local intensity variation in the presence of noise. The experiments show that the proposed method delivers high denoising performance, both in terms of objective metric and the visual quality.*

Keywords: Diffusion, Patch, Region, Over-segmentation.

1. Introduction

Nonlinear anisotropic diffusion has drawn considerable attention over the past decade and has experienced significant developments as it gracefully diffuses the noise in the intra-region while inhibiting inter-region smoothing. Introduced first by Perona and Malik (PM diffusion) [1] the diffusion process is mathematically described by the following equation:

$$\frac{\partial}{\partial t} I(x,y,t) = \nabla \bullet (c(x,y,t)\nabla I) \quad (1),$$

where I(x,y,t) is the image, t is the iteration step and $c(x,y,t)$ is the diffusion function monotonically decreasing of the magnitude of the image gradient. Two diffusivity functions proposed are:

$$c_1(x,y,t) = \exp\left(-\left(\frac{|\nabla I(x,y,t)|}{\lambda}\right)^2\right) \quad (2)$$

and

$$c_2(x,y,t) = \frac{1}{1+\left(\frac{|\nabla I(x,y,t)|}{\lambda}\right)^2} \quad (3),$$

where λ is referred to as a diffusion constant. Depending on the choice of the diffusivity function, equation (1) covers a variety of filters. The discrete diffusion structure is translated into the following form:

$$I_{i,j}^{n+1} = I_{i,j}^{n} + (\nabla t) \bullet \left[\begin{matrix} c_N\left(\nabla_N I_{i,j}^n\right) \bullet \nabla_N I_{i,j}^n + c_S\left(\nabla_S I_{i,j}^n\right) \bullet \nabla_S I_{i,j}^n + \\ c_E\left(\nabla_E I_{i,j}^n\right) \bullet \nabla_E I_{i,j}^n + c_W\left(\nabla_W I_{i,j}^n\right) \bullet \nabla_W I_{i,j}^n \end{matrix} \right] \quad (4),$$

Subscripts N, S, E and W (North, South, East and West) describe the direction of the local gradient, and the local gradient is calculated using nearest-neighbor differences as

$$\nabla_N I_{i,j} = I_{i-1,j} - I_{i,j}; \quad \nabla_S I_{i,j} = I_{i+1,j} - I_{i,j}$$
$$\nabla_E I_{i,j} = I_{i,j+1} - I_{i,j}; \nabla_W I_{i,j} = I_{i,j-1} - I_{i,j} \quad (5).$$

Generally, the effectiveness of the anisotropic diffusion is determined by (a) the efficiency of the edge detection operator to distinguish between noise and edges; (b) the accuracy of an "edge-stopping" function to promote or inhibit diffusion; and (c) the adaptability of a convergence condition to terminate the diffusion process automatically. The model in [1] has several practical and theoretical limits. It needs a reliable estimate of image gradients because with the increase of the noise level, the effectiveness of the gradient calculation degrades and deteriorates the performance of the method. Secondly, the equal number of iterations in the diffusion of all the pixels in the image leads to blurring of textures and fine edges.

Several authors have independently proposed modifications to the model to overcome the above problem. Catte et al. [2] used a smoothed gradient of the image, rather than the true gradient. The smoothing operator removes some of the noise which might have deceived the original PM filter. In this case, the scale parameter σ is fixed. In [3] authors have proposed the

inhomogeneous anisotropic diffusion which includes a separate multiscale edge detection part to control the diffusion.

Yu et al. [4] proposed a method wherein the SUSAN edge detector is incorporated into the model. Noise insensitivity and structure preservation properties of SUSAN guides the diffusion process in an effective manner. Li et al. [5] proposed a context adaptive anisotropic diffusion via weighted diffusivity function by jointly exploiting contextual information (i.e. calculation of gray level variance) and spatial gradient. Chao and Tsai [6] proposed a diffusion model which incorporates both the local gradient and the gray-level variance to preserve edges and fine details while effectively removing noise. When the level of noise is high; noisy pixels in the image generally involve larger magnitudes of gray level variance and gradients than those of actual edges and fine details. Thus, the method is becoming inefficient quite soon. Wang et al. [7] proposed a local variance controlled scheme wherein spatial gradient and contextual discontinuity of a pixel are jointly employed to control the evolution. However, a solution to estimating the contextual discontinuity leads to an exhaustive search procedure, which causes algorithm to be too computationally expensive. Zhang et al. [8] presented a Laplacian pyramid-based nonlinear diffusion (LPND) method where Laplacian pyramid was utilized as a multiscale analysis tool to decompose an image into subbands, and then anisotropic diffusion with different diffusion flux is used to suppress noise in each subband. LPND tries to introduce sparsity and multiresolution properties of multiscale analysis into anisotropic diffusion. Another approach to context-based diffusion was researched in [9], where we proposed SWCD method. The multi-scale stationary wavelet analysis of the local neighborhood across the scales provides the edge information partially free of noise and thus makes possible the tunable diffusion. As a result, and due to the shift invariance property of stationary wavelet transform the PSNR has been improved compared to Shih's diffusion [10] which was performed on wavelet coefficients without consideration of the structural content of the local neighborhood.

State-of-the art denoising techniques all rely on patches, either for dictionary learning [11,12], collaborative denoising of blocks of similar patches [13] or for non-local sparse models [14]. Regularization with non-local patch-based weights has shown improvements on classical regularization involving only local neighborhoods [15, 16, 17]. The shape and size of patches should adapt to anisotropic behaviour of natural images [18, 19]. In spite of the high performance of the patch-based denoising techniques they generally produce artifacts even at a comparatively moderate noise levels. In addition, the size of the patch has a significant impact on the PSNR even for the similar or identical contents.

All above considerations suggest an approach which incorporates adaptation to the image local structure within optimally sized patches. Unlike block-transform based methods such as BM3D [15] which perform with a pre-determined optimum block size and clustering-based denoising methods such as KLLD [14] which uses a predetermined optimum number of classes, our method searches for an optimum patch size through iterative diffusion starting with a small patch size, that is a large number of patches and proceeds with a smaller number of patches, that is large patches until a best PSNR is attained and no further improvement is possible. To initialize the algorithm we use superpixel segmentation [20]. Each superpixel is diffused to the best PSNR, and then the process iterates on larger superpixels. In our pursuit of determining the local gradient and thus an amount of diffusion we use the inverse difference moment (IDM) feature [23]. We demonstrate that the feature is robust in determining the amount of local intensity variation in the presence of noise. Overall the diffusion process converges to PSNR levels known by the state-of-the-art methods with a minimum visible blocking/patching artifacts. The method is called feature based locally adaptive diffusion (FLAD) method.

The rest of the paper is organized as follows: Section 2 provides a theoretical background and introduces the method and implementation details. Section 3 presents results of the experiment; thereafter we conclude.

2. Feature Based Locally Adaptive Diffusion (FLAD)

2.1 Superpixel Segmentation

As it was pointed out earlier in this paper, we need the image to be over-segmented first. For this purpose we use superpixel segmentation. A single parameter of the method- k is a desired number of approximately equally-sized superpixels. The procedure begins with an initialization step where k initial cluster centers C_i are sampled on a regular grid spaced S pixels apart. To produce roughly equally sized superpixels, the grid interval is $S = \sqrt{N/k}$. The centers are moved to seed locations corresponding to the lowest gradient position in a 3x3 neighborhood, and thus avoid centering a superpixel on an edge. This reduces the chance of seeding a superpixel with a noisy pixel. Next, in the assignment step, each pixel i is associated with the nearest cluster center whose search region overlaps its location. A distance measure D, determines the nearest cluster center for each pixel. Since the expected spatial extent of a superpixel is a region of an approximate size SxS, the search for similar pixels is carried in a region of size $2Sx2S$ around the superpixel center. Once each pixel has been associated to the nearest cluster center, an update step adjusts the cluster centers to be the mean vector of all the pixels belonging to the cluster. The $L2$ norm is used to

compute a residual error *E* between center locations of the new and the previous clusters. The assignment and update steps can be repeated iteratively until convergence. Experimentally, twenty iterations are sufficient for most images, and therefore throughout the rest of the paper we use this value.

2.2. Modified Diffusion

Mentioned above the normalized inverse difference moment (IDM) feature is visualized in Fig.1. The feature captures texture details in both coarse and fine structures. IDM will get small contributions from homogenous region and larger values in non-homogenous regions. Ranging between 0 and 1; the feature being 0 has an indication of a pixel being a part of a homogenous neighborhood. The value being 1 indicates that the pixel is a part of texture or an object boundary.
The diffusivity function of Eq.2 is modified to the following:

$$c_p = \exp\left(-\left(\frac{IDM(I)}{\lambda}\right)^2\right), p = N, S, W, E$$

,

where

$$IDM = 1 - \sum_{i=0}^{G-1}\sum_{j=0}^{G-1}\frac{1}{1+(i-j)^2}P(i,j)$$

Given an MxN neighborhood containing G gray levels from 0 to G-1, let f(m,n) be the intensity at sample m, line n of the neighborhood.

Then

$$P(i, j \mid \Delta x, \Delta y) = W \cdot Q(i, j \mid \Delta x, \Delta y)$$

,

Where

$$W = \frac{1}{(M-\Delta x)(N-\Delta y)};$$

$$Q(i, j \mid \Delta x, \Delta y) = \sum_{n=1}^{N-\Delta y}\sum_{m=1}^{M-\Delta x} A$$

and

$$A = \begin{cases} 1, iff\,(m,n) = i \quad and \quad f(m+\Delta x, n+\Delta y) = j \\ 0, elsewhere \end{cases}$$

For calculation we use 9x9 window centered at pixel(i,j).

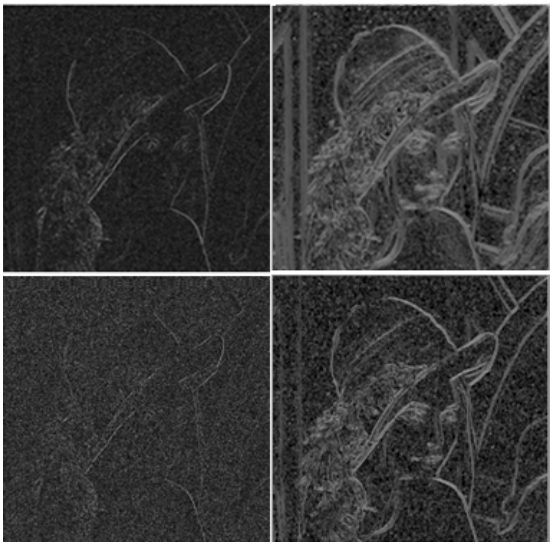

Fig.1 1st column: Gradient image for additive white Gaussian noise level σ =20, 40 for "Lena"; 2nd column: Inverse difference moment for additive white Gaussian noise level σ =20, 40

2.3 FLAD Algorithm

Let us denote *I* - input image, k – number of regions, *m* – number of merging steps, *Var* –intensity variance and *n* – number of diffusion steps. The method performs according to the following steps:

1. *Initialize m=0, α = 1.1, λ =10. Segment image into k (k≠1) regions.*
2. *Initialize n=0. Calculate PSNR for each region of initial partition, i.e., $[PSNR_k^{(0)}]_0$.*
3. *Iteration step: Diffuse image pixel $I_{i,j}$ using Eq.(4).*
4. *For $\forall R_i$: if $[PSNR_k^{(n+1)}]_m > [PSNR_k^{(n)}]_m$, Goto Step 3; else Goto Step 6.*
5. *While $R_m \neq I$, for $\forall$ Ri ~ Rj, if $Var(R_j) \leq \alpha * Var(R_i)$, then $R_i \cup R_j$; m=m+1; update k;, Goto Step 2, else Repeat Step 5 with $\alpha = \alpha + 0.1$.*
6. *Stop.*

3. Experimental Results

We now test the proposed method on the benchmark images corrupted by additive white Gaussian noise. Initial number of superpixel segments is set to 'k' = MxN/patch size; where MxN is the size of the image and the patch size is usually set globally (between 5x5 and 19x19). In our work, we calculate the bounds with the patch size of 8x8 for low noise levels i.e. σ≤40 and a larger patch size such as 11x11 for high noise levels i.e. σ>40. The diffusion constant $\lambda = 10$ in the evaluation of benchmark images with σ=10, 20, 30, 50 and 100 of the additive white Gaussian noise. Table I provides PSNR values by

Table I. PSNR of the proposed method.

Image/Noise, σ	FLAD				
	10	**20**	**30**	**50**	**100**
Lena	35.56	32.61	30.85	28.59	25.56
House	35.94	32.93	31.11	28.68	25.12
Peppers	34.48	31.05	29.03	26.56	23.18
Cameraman	33.99	30.18	28.24	25.89	23.08

Fig.2. First row: “Lena” image and Lena with additive white Gaussian noise level σ =100; Second row: results by BM3D and FLAD

Table II. PSNR comparison of different anisotropic diffusion methods for "Lena".

Method/ σ	10	15	20
Noisy	28.15	24.62	22.14
PM [1]	32.70	30.71	29.37
Catte [2]	33.27	31.39	30.09
Li [5]	34.28	32.41	31.15
GSZ FAB [21]	32.49	29.86	28.29
LVCFAB [7]	31.90	28.21	26.67
RAAD [22]	34.33	32.53	31.24
FLAD	**35.56**	**33.86**	**32.61**

Fig.3. First Column: "Lena" image with additive white Gaussian noise level σ =20 and 50; Second Column: corresponding results by FLAD

the proposed method for benchmark images. Second, the proposed FLAD algorithm is compared to six diffusion based methods which are considered as the state-of- the-art techniques in diffusion based denoising, which are FAB based diffusion, GSZ FAB [21], LVCFAB [7], and RAAD [22]. The improvement by FLAD for the given noise levels is ranging from 1.3 dB for low noise to 1.59dB for noise level with σ=100. Finally, the comparison to BM3D is due, and it shows that the performance of FLAD is 0.35 dB lower compared to that of the BM3D for noise level σ=10 and 0.39 dB lower for noise level σ=100. Fig.2 shows that lesser or no blocking/ringing artifacts are introduced by FLAD compared to those in BM3D denoised images. The denoising performance of the FLAD is further illustrated in Fig.3, where we show fragments of a few noisy (σ=20 and 50) test images and fragments of the corresponding denoised ones. The denoised images show high visual quality in the areas of smooth intensity transition and lesser or no ringing around contours of extended objects.

4. Conclusion

We have presented a novel FLAD algorithm for image denoising. The high performance of the method is attained due to the following properties: a) patch-based optimization of PSNR through iterative diffusion; b) agglomeration of patches and repetitive iteration of the process; c) modification of the diffusion function. The method has attained a highest performance in the class of advanced diffusion based methods and outperforms its counterpart by reducing visible blocking and ringing artifacts inherent to block- and transform-based methods.

Acknowledgement

This material is based upon work supported by NASA EPSCoR under Cooperative Agreement No. NNX10AR89A.

References:

1. P. Perona and J. Malik, “Scale-space and edge detection using anisotropic diffusion,” IEEE Transactions on Pattern Analysis and Machine Intelligence, vol. 12, no. 7, pp. 629–639, 1990.
2. F. Catté, P.-L. Lions, J.-M. Morel, and T. Coll, “Image selective smoothing and edge detection by nonlinear diffusion,” SIAM Journal on Numerical Analysis, vol. 29, no. 1, pp. 182–193, 1992.
3. V. B. Surya Prasath and Arindama Singh, “Well-Posed Inhomogeneous Nonlinear Diffusion Scheme for Digital Image Denoising,” Journal of Applied Mathematics, vol. 2010, Article ID 763847, 14 pages, 2010. doi:10.1155/2010/763847
4. Jinhua Yu, Jinglu Tan, Yuanyuan Wang. Ultrasound speckle reduction by a SUSAN-controlled anisotropic diffusion method. Pattern Recognition, 2010: 3083-3092.
5. H. C. Li, P. Z. Fan, and M. K. Khan, “Context-Adaptive Anisotropic Diffusion for Image Denoising,” IET Electronics Letters, vol.48, no.14, pp.827-829, 2012.
6. Shin-Min Chao, Du-Ming Tsai: An improved anisotropic diffusion model for detail- and edge-preserving smoothing. Pattern Recognition Letters 31(13): 2012-2023 (2010).
7. Y. Wang, L. Zhang, P. Li. Local Variance-Controlled Forward-and-Backward Diffusion for Image Enhancement and Noise Reduction. IEEE Transactions on Image Processing, 2007: pp.1854-1864.
8. Zhang Fan, Mo Yoo Yang, Mong Koh Liang, and Kim Yongmin, "Nonlinear Diffusion in Laplacian Pyramid Domain for Ultrasonic Speckle Reduction," IEEE Trans. Med. Imaging. 26, 200-211 (2007).
9. Ajay K. Mandava and Emma E. Regentova, “Image denoising based on adaptive nonlinear diffusion in wavelet domain”, J. Electron. Imaging 20, 033016 (Sep 14, 2011)
10. Shih, A.C.-C., Liao, H.-Y.M., Lu, C.-S.: A New Iterated Two-Band Diffusion Equation: Theory and Its Applications. IEEE Transactions on Image Processing (2003) DOI: 10.1109/TIP. 2003.809017.
11. M. Aharon, M. Elad and A. M. Bruckstein, “The K-SVD: An Algorithm for Designing of Overcomplete Dictionaries for Sparse Representation,” IEEE Transactions on Signal Processing, Vol. 54, No. 11, 2006.
12. P. Chatterjee and P. Milanfar, Clustering-based Denoising with Locally Learned Dictionaries (K-LLD), IEEE Transactions on Image Processing, vol. 18, num. 7, July 2009, pp. 1438-1451
13. K. Dabov, A. Foi, V. Katkovnik, and K. Egiazarian, “Image denoising by sparse 3D transform-domain collaborative filtering,” *IEEE Trans. Image Process.*, vol. 16, no. 8, pp. 2080-2095, August 2007.
14. J. Mairal, F. Bach, J. Ponce, G. Sapiro, and A. Zisserman, "Non-Local Sparse Models for Image Restoration," *Proc. of ICCV*, September-October 2009.
15. Gilboa, G., Osher, S.: Nonlocal operators with applications to image processing. Multiscale Model. Simul. **7**(3), 1005-1028 (2008).
16. Peyre, G., ″Image Processing with Non-Local Spectral Bases″ SIAM *Journal on* Multiscale. Modeling and Simulation 7, 2 *(2008) 703-730.*
17. X. Zhang, M. Burger, X. Bresson, and S. Osher, "Bregmanized Nonlocal Regularization for

Deconvolution and Sparse Reconstruction", SIAM Journal on Imaging Sciences, 3(3), 253-276, 2010

18. K. Dabov, A. Foi, V. Katkovnik, and K. Egiazarian, “A nonlocal and shape-adaptive transform-domain collaborative filtering”, Proc. Int. Workshop on Local and Non-Local Approx. in Image Process., LNLA 2008, Lausanne, Switzerland, August 2008.
19. Charles-Alban Deledalle, Vincent Duval and Joseph Salmon, *Non-Local Methods with Shape-Adaptive Patches (NLM-SAP)*, Journal of Mathematical Imaging and Vision, pp. 1-18, 2011
20. Achanta, R.; Shaji, A.; Smith, K.; Lucchi, A.; Fua, P.; Süsstrunk, S.; , "SLIC Superpixels Compared to State-of-the-Art Superpixel Methods," *Pattern Analysis and Machine Intelligence, IEEE Transactions on* , vol.34, no.11, pp.2274-2282, Nov. 2012
21. G. Gilboa, N. Sochen, and Y. Y. Zeevi, “Forward-and-backward diffusion processes for adaptive image enhancement and denoising,” *IEEE Trans. Image Process.* **11**(7), 689–703 (2002).
22. Y. Wang , R. Niu , L. Zhang and H. Shen "Region-based adaptive anisotropic diffusion for image enhancement and denoising", *Opt. Eng*. 49(11), 117007 (2010).
23. Cooper, G.R.J., “The Antialiased Textural Analysis of Aeromagnetic Data”, Computers & Geosciences v.35, p.586-591 (2009).